Nanostructure La doped NiO prepared by green method and their luminescence applications

[1]Lakshmikanth Reddy and [2]Siva Yellampalli
[1]Dept. of Electrical & Electronics Engineering, Acharya Institute of Technology, Soldevanahalli, Bangalore -107.
[2]VTU Extension Center, UTL Technologies Ltd., Bangalore-22.

Abstract: The Nickel oxide (NiO) (L1) and Lanthanum doped NiO nanoparticles (La doped NiO NPs) (L2) were prepared by Green method. To determine the effect of La doping with Nickel oxide, an appropriate amount of La ions were incorporated with NiO matrix. The green synthesized NiO and La doped NiO NPs structural, phase, morphological, chemical composition, functional group and optical properties were investigated by XRD, XPS, FESEM, EDAX, FT-IR and Photoluminescence spectroscopy.

I. Introduction

The electronic and memory device consumption in the manufacturing process leads to a huge amount of surplus electrical and electronic waste dumped on all over the world. Gallium and indium semiconducting material are used in electrical and electronic circuits and availability for about 30 years. So there is a need to control the resource exploitation and the electronics, so that the environmental risks are minimized that will result in a sustainable future. To develop the goal of sustainability in the electronics field, we can introduce eco-friendly materials namely "Green materials". For the green materials to be highly abundant, the organic precursors must be of low cost and avoid the use of toxic solvents. Chemically synthesized nanoparticles are highly toxic and lead to non-eco-friendly by-products [1]. Biological approaches using plants or plant extracts for metal oxide nanoparticles have been suggested as valuable alternatives to chemical methods.

The NiO NPs are significant important semiconductor materials, which can be widely studied in the recent years and wide band gap (3.6-4.0eV) p-type semiconductor[2], potentially used in many applications, such as lithium ion batteries, solar cells, electro-chromic coatings, fuel cells, antiferromagnetic, smart windows, super-capacitors, gas sensor and dye-sensitized photo cathodes [3,4].

Lanthanum doped nanoparticles are potentially important for optoelectronics, luminescence and others application. The transitions play significant roles in the absorption of rare earth metal ions in the UV range. The electron transfers process from semiconductor host material to doping with lanthanum atoms stimulates the doped nanoparticles. An energy transfer process from the excited semiconductor host to doping lanthanide atoms stimulated to absorption of optically centres and enlargement of luminescent and Photo degradation properties [5,6].

In the present work, NiO and La doped NiO NPs prepared through green eco-friendly method using *Azadirachta indica* leaf extract. The synthesized nanoparticles were characterized by structural, morphological, chemical and optical studies carried out.

II. Materials and method

The freshly collected *A. Indica* leaf was washed several times with de-ionized water to remove the adhering foreign impurities. The aqueous leaf extract (ALE) was prepared by taking, 10 gms of fresh leafboiled at a temperature of 80 ˚C in 100 ml of double distilled water for 15 mins. Further leaf extract was filtered usingwhatman no. 1 filter paper.

For synthesis of i) NiO (L1) NPs, the 0.1 M of Nickel (II) nitrate salt and ii) La doped NiO NPs, 0.002 M of Lanthanum (III) nitrate and 0.098 M of Nickel (II) nitrate salt (L2) were dissolved in ALE solution.The ALE Nickel nitrate both solutionswere heatedat 80˚C for 6 hrs using a reflux condenser to avoid the solved evaporation. After 6hrs, both the solutions were brought back to room temperatureand evaporatedat120˚C to remove the moisture. Following that, the precipitates (green colour) of NiO and NiLaO NPs were annealed at 800˚C for 5 hrs (turned into black colour).

The resulting NiO and La doped NiO NPs was subjected to different characterization techniques: X-ray diffraction pattern using X'PERT PRO PAN analytical, measured in the range between 20^{o} - 80^{o} at source CuKα (1.54 Å) was used. The oxidation state and surface functionalization of the materials were identified by XPS measurement.The topography and elemental composition were observed from FESEM with EDAX (Carl Zeiss Ultra 55FESEM and Inca: EDAX). The functional group analysis was studied using

Fourier transform infra-red spectra recorded in the range 4000-400 cm^{-1}. The photoluminescence (PL) measurement was carried out by using Cary Eclipse spectrometer.

III. Results and discussions

The *A. Indica* leaf contained various phytochemical components suchalkaloids, flavonoids, triterpenoids, phenolic compounds, carotenoids, steroids, and ketones etc., [7]. The Neem leaf extract Phyto-components are reducing agent to synthesis NiO NPs. The Phytochemicals constituent converts as nickel nitrate ($Ni(NO_3)_2$)to nickel hydroxide ($Ni(OH)_2$) NPs. This $Ni(OH)_2$NPs were heatedat 120°C to remove the water molecules finally annealing at 800 °C for 5 h, is converted into NiO NPs.The synthesis formation of NiO NPs has shown in Fig. 1.

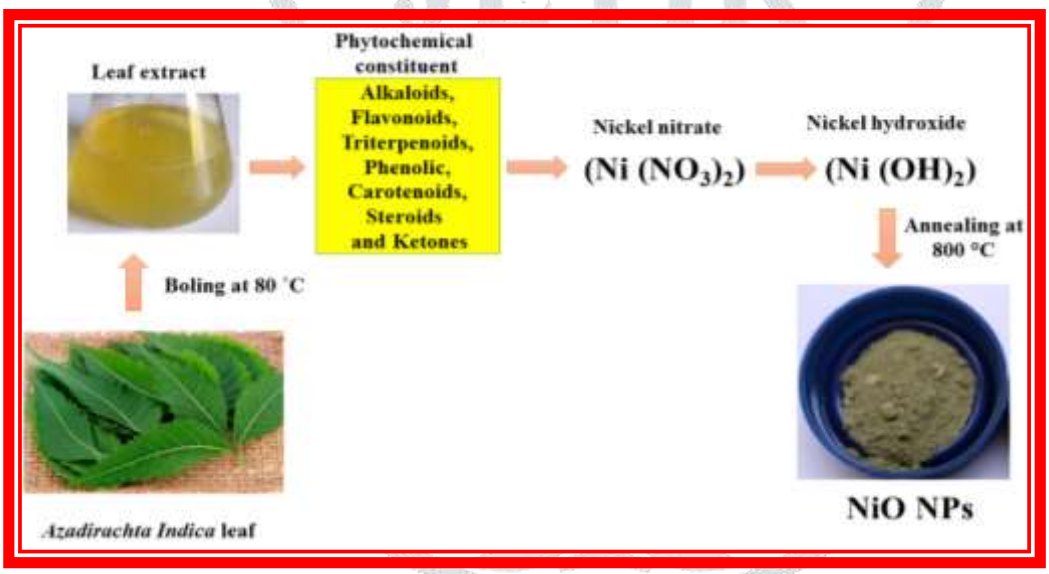

Figure 1 shows graphical representation of NiO NPs formations.

The XRD patterns of green synthesized L1and L2 samples are shown in Fig.2. The synthesized nanoparticles are indicating that the high intense and well-define crystalline nature of samples. The noticeable XRD peaks of L1 sample were observed at 37.35˚, 43.38˚, 62.94˚, 75.47˚ and 79.46˚ and corresponding to the hkl planes are (111), (200), (220), (311) and (222) respectively. The diffraction peaks displays the face centre cubic phase of NiO NPs, as confirmed through the JCPDS card no. 36-1451. Figure 3(a-b) shows that the La doped NiO samples retain same crystal structure of NiO, which results La doping has not changed in the crystal structure of NiO NPs, but slight higher angle shift observed in the 2θ angles

due to the substitution of La^{3+} ions into the NiO matrix. The lattice constant and unit volume value are estimated at(4.1696 Å and 4.1701 Å) and (72.49 $Å^3$ and 72.51 $Å^3$) for L1and L2 samples respectively may be due to the La doping effects of increasing the lattice parameter values. The average crystallite sizes are observed at 57.12 nm and 47.72 nm for L1 and L2 samples respectively, reduction may be substitution La^{3+} ions NiO matrix.

The lattice strain may be substitution of La^{3+} ions in the crystal structure of NiO NPs and the crystallite size were calculated by the Williamson-Hall (W-H) relation [8]. The strain values are 0.00105 and 0.00171 for L1 and L2 samples (Fig. 4(a-b)) respectively, increasing the strain in the L2 sample as compared to the L1 sample. This can be modification of the electrostatic interactions between ions along various planes. This may be due to the different oxidation states of lanthanum and Nickel ions.

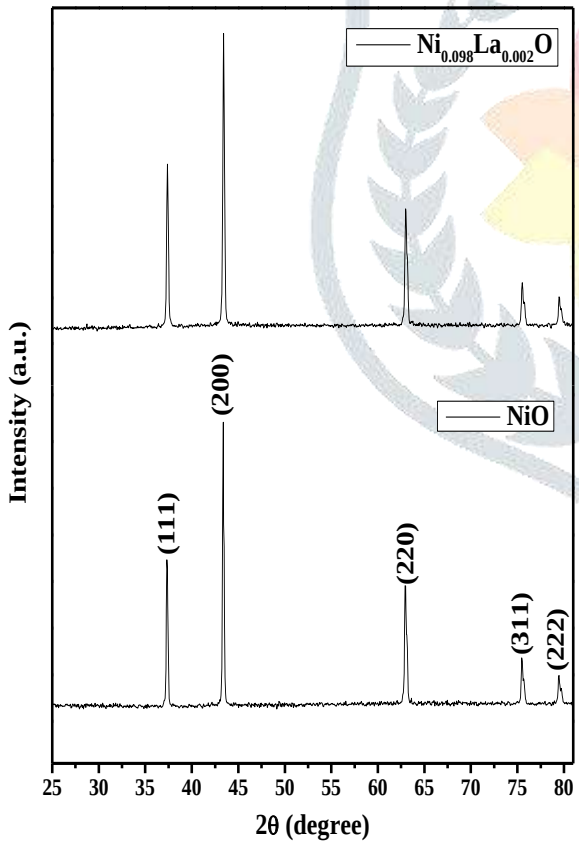

Figure 2 X-ray diffraction pattern of NiO and La doped NiO NPs.

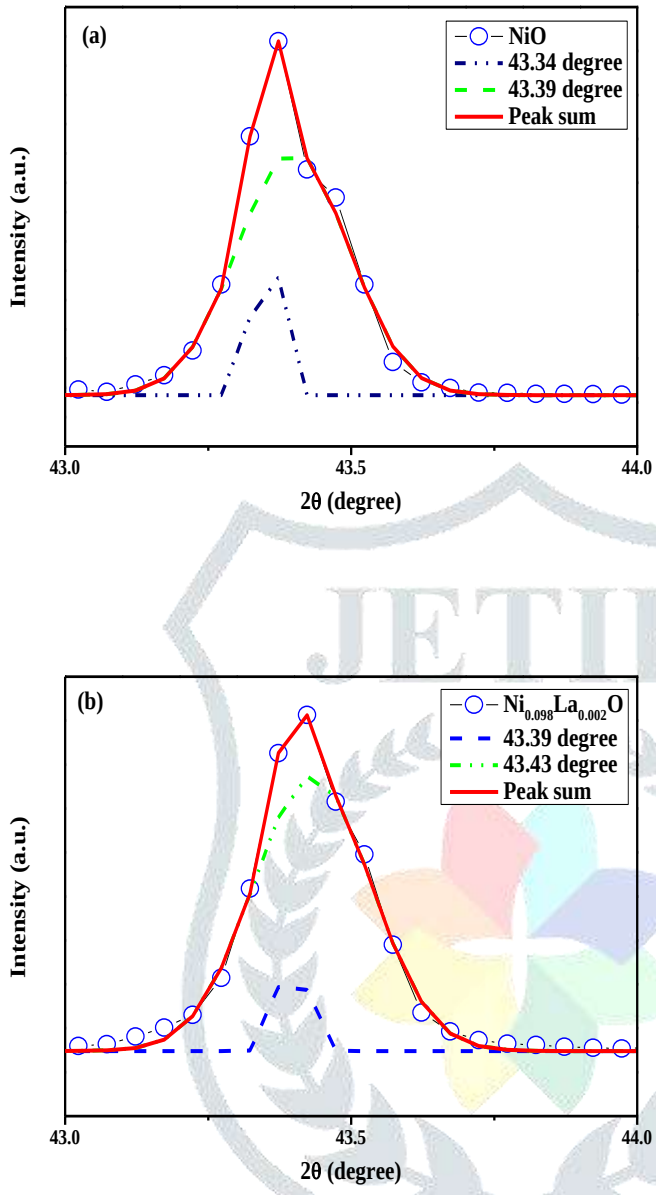

Figure 3(a-b) shows the doping induced peak shift of XRD patterns.

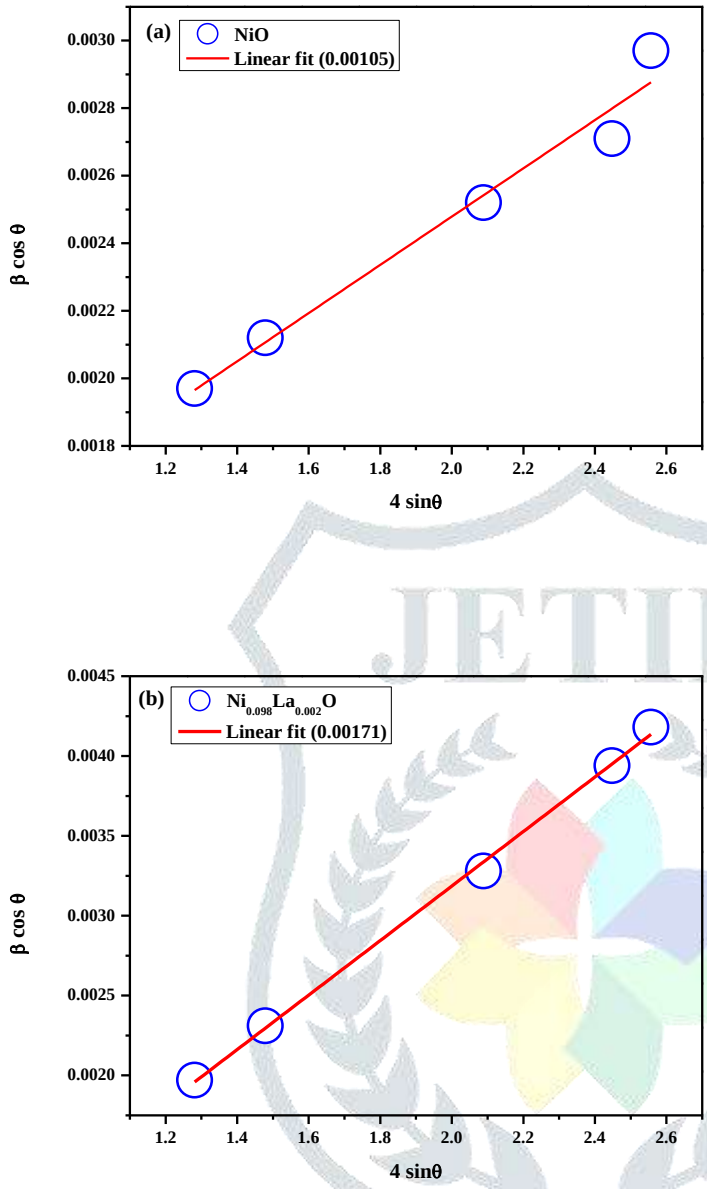

Figure 4 William-Hall plot analysis of (a) NiO and (b) La doped NiO NPs.

XPS studies indicate that characteristic oxidation date of Ni (2p), La (3d) and O (1s) are present in Fig. 5 (a-c) and 6(a-d). Figure 5a and 6a shows that XPS wide spectrum of NiO and La doped NiO NPs. The Ni (2p) oxidation state are decomposed into seven and nine peaks observed at (882.34 eV, 875.12 eV, 863.65 eV, 860.07 eV, 857.30 eV and 854.44 eV)(879.71 eV, 872.40 eV, 870.94 eV, 865.55 eV, 860.55 eV, 856.85 eV, 855.88 eV, 854.18 eV) for L1and L2 samples respectively. The Ni (2p) state split into Ni ($2p_{3/2}$) and Ni ($2p_{1/2}$) are observed from ((854.44 – 857.30 eV) & (854.18 – 856.85 eV)) and ((875.12 eV) &

(870.94 – 872.40 eV) for NiO and La doped NiO NPs respectively. Further the Ni ($2p_{3/2}$) and Ni ($2p_{1/2}$) state satellite peaks are found to be ((860.07 - 863.65 eV) & (860.55 - 865.55 eV)) and ((882.34 eV) & (879.71 eV)) for respective NiO NPs. These Ni ($2p_{3/2}$), Ni ($2p_{1/2}$) and satellite peaks is ascribed to Ni^{2+} of NiO NPs, Ni^{2+} of Ni $(OH)_2$ and Ni^{2+} of NiO (satellite) respectively [9,10]. The binding energy values of L2 decreased than the L1 samples, which is attributed to the La^{3+} ions incorporation of NiO matrix, lanthanum ions does not affected the Ni phase of NiO NPs.

The O (1s) signals of L1 and L2 samples (Fig. 5b and 6b) are deconvoluted into doubled pair at (529.87 & 533.18 eV) and (529.39 & 531.14 eV)respectively. First peak observed at 529.87 eV and 529.39 eV are attributed to lattice oxygen (O^{2-}) of NiO NPs. Second peak located at 533.18 eV and 531.14 eV, which is due to the hydroperoxy group (-OOH) and chemisorbed oxygen on surface respectively [11, 10]. In early literature, the binding energy values (529.7, 530.9, 531.8, 532.8 and 533.7 eV) of NiO NPs of O (1s) signal decreased as compared to (529.4, 530.4, 531.2, 532.0,533.0 and 533.8 eV) NiO NPs, this effects enhanced the gas sensing properties [10]. Our XPS results also same trend exhibits for La doped NiO NPs, so that we suggested that La doped NiO NPs are effectively may work as gas sensor.

In the case of La doping (Fig 6d), the La 3d signals are deconvoulated at seven peaks at 864.99 eV, 861.00 eV, 855.23 eV, 853.71 eV, 851.24 eV, 838.99 eV and 834.63 eV, respectively. The La (3d) signal split into La $3d_{5/2}$and La $3d_{3/2}$located at (834.63 & 838.99 eV) and (851.24, 853.71 and 855.23 eV), respectively [12].

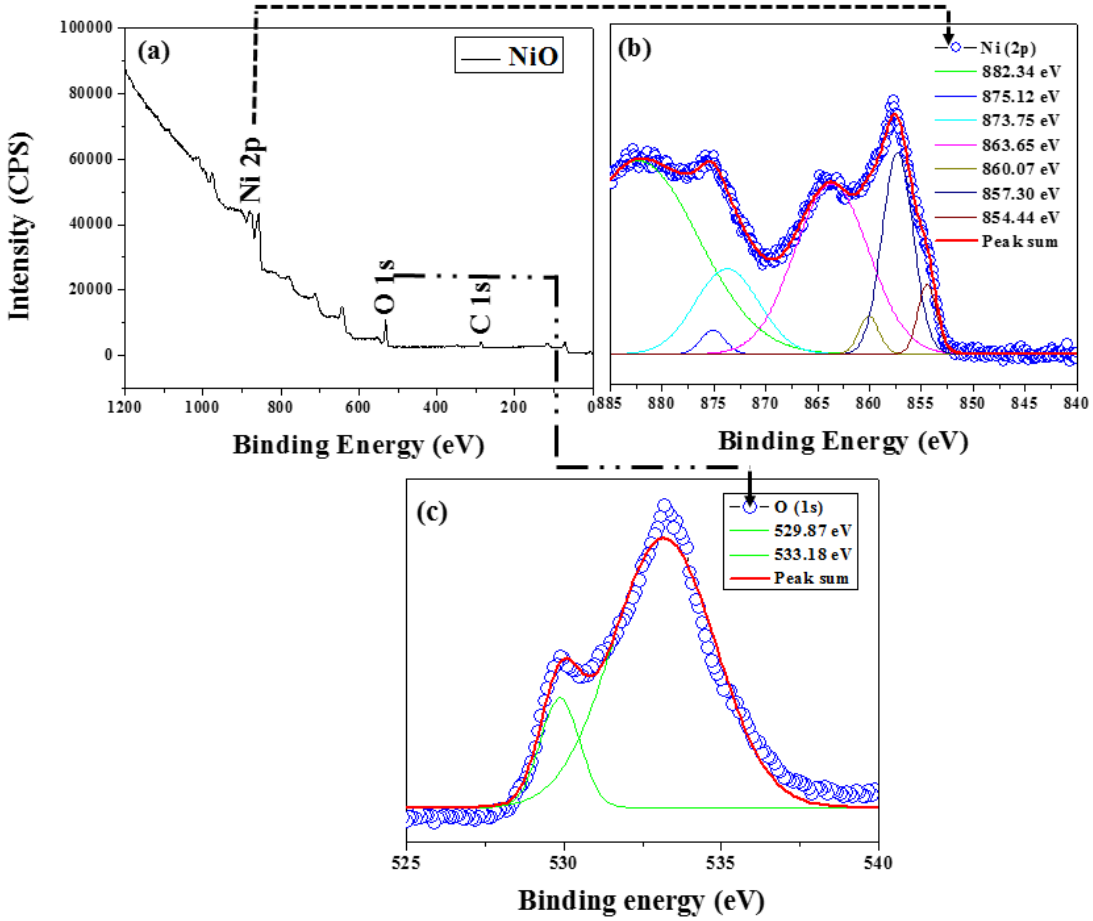

Figure 5 XPS spectra of (a) wide spectra, (b) Ni (2p) and (c) O (1s) oxidation state of NiO NPs.

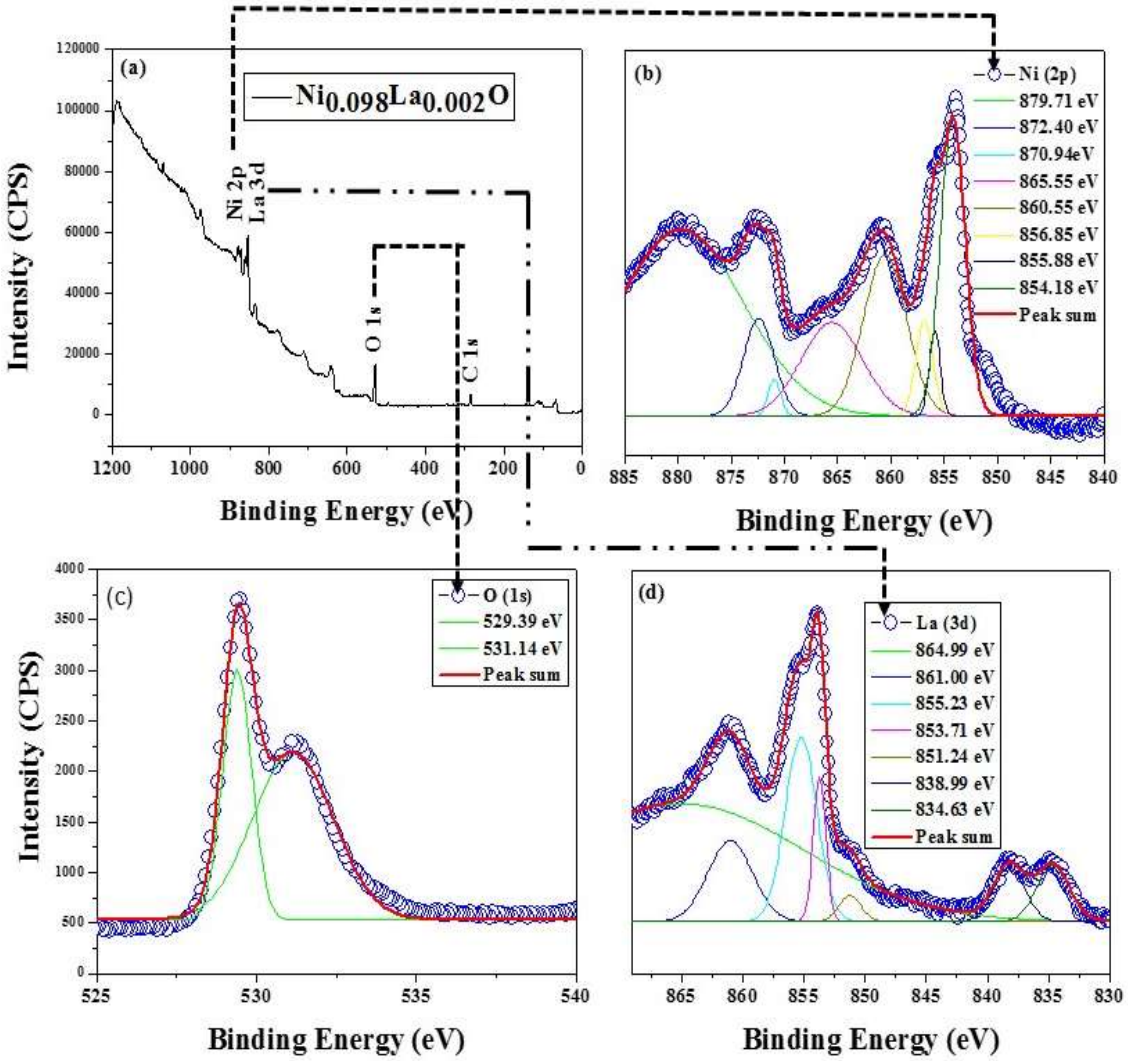

Figure 6 XPS spectra of (a) wide spectra, (b) Ni (2p), (c) O (1s) and La (3d) oxidation state of La doped NiO NPs.

Figure7 (a-b & d-e) shows that the FESEM image of L1 and L2 samples. The L1 and L2 samples are formed uniform spherical and trigonal structure and average particle size range between 30-100 nm. The nanoparticles morphology formation occurs slight space in between the nanoparticles and the porous formation observed in nanostructure. The more porous formationis observedL2 sample as compared to the L1 sample. In early literature, the nanostructure porous formation plays a critical role in the performance of sensor activity, because of large surface area, which may be increasing the rate of gas diffusion [13]. In the case La doped NiO NPs has more porous present than NiO NPs. Hence our green synthesized La doped NiO NPs are surely used in hazards gas sensing applications.

The atomic percentage of element constituent was identified by EDAX spectra. The chemical composition of the L1 and L2 samples are represented in Fig. 7 (c and f).This result confirms that La, Ni and O elements are present in the samples and metal La, Ni and O elemental peaks are observed at normal energy level. From the EDAX spectra, the various area position of the sample was chosen and scanning, the same lanthanum content was present, and it's proposed that lanthanum elements uniform distribution on NiO matrix. In the present result, the lanthanum (la) atomic percentage is found to be 1.58 % for La doped NiO NPs. The Ni and O elements atomic percentage are observed at (60.88% and 39.12%) and (40.20% and 50.22%) for NiO and La doped NiO NPs, respectively. The doped sample oxygen percentage increased and Nickel percentage decreased, this may be a local lattice strain due to La doping effects.

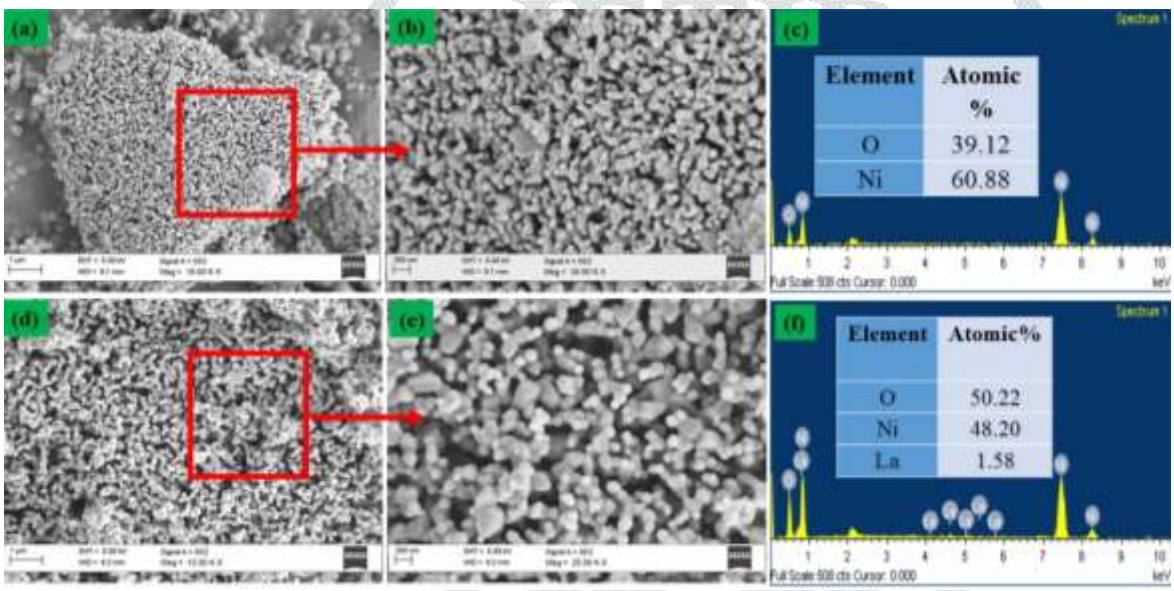

Figure 7(a-f) FESEM and EDAX spectra of NiO and La doped NiO nanostructures.

The *A. Indica* leaf extract contribution of the phyto-compounds using to synthesized *NiO* and La doped NiO NPs were confirmed by FTIR spectra Fig. 8. The green synthesis NiO and La doped NiO NPs different IR bands are observed at (3433, 2924, 1633, 1107, 499 and 441 cm-^{1}) and (3435, 2925, 1346, 1102,486 and 422 cm^{-1}), respectively. The wide (O-H) stretching bands are observed at (3435 and 3435 cm^{-1}) for NiO and La doped NiO NPs, which is generally linked with phenols and carboxylic acids. The C-H stretching bands located at 2924 and 2925 cm^{-1} for respective NiO NPs are attributed to alkenes/aldehydes. The NiO and La doped NiO NPs other function groups are 1633 cm^{-1} (C-C) aromatic stretching, 1346 cm^{-1}

(C-H) alkenes rocking structure. The Ni-O (Metal – oxide) stretching bands are centred at (499 and 441 cm-[1]) and (486 and 422 cm^{-1}) for NiO and La doped NiO NPs respectively. This result shows indicated that phytochemical component is associated with biotransformation of nickel nitrate salts converted to NiO NPs, this phytochemical component generally act as an oxidation agent during nanoparticles formation [14].

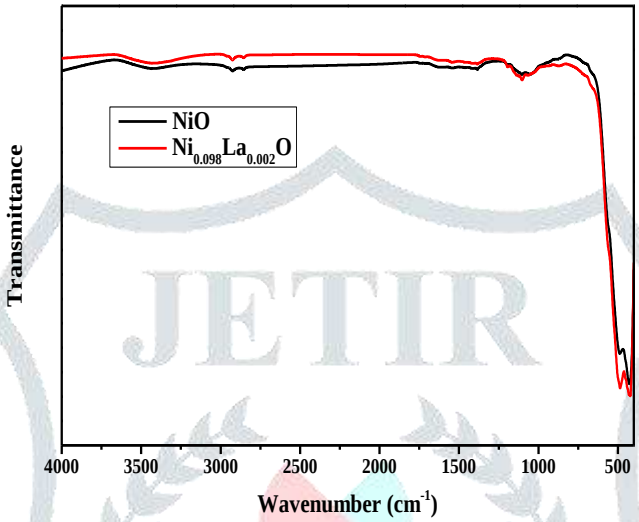

Figure 8 FTIR spectra of NiO and La doped NiO NPs.

The PL spectra of green synthesized NiO and La doped NiO NPs observed at the excitation wavelength of 300 nm is shown in Fig 9 (a-b). The PL spectra of Gaussian decomposition peaks position observed at (360 nm, 393 nm, 411 nm, 452 nm and 487 nm) and (353 nm, 391 nm, 405 nm and 452 nm) for NiO and La doped NiO NPs respectively. The PL spectra UV region (360 nm & 393 nm) and (353 nm & 391 nm) resemble to near band edge (NBE) emission, which is due to the electronic transitions of the Ni^{2+} ion. The violet bands cantered at 405 nm and 411 nm are attributed to the radiating defects like nickel interstitials [15,16]. The blue bands located at (452nm & 487 nm) and (452 nm) for NiO and La doped NiO NPs respectively is attributed to the surface oxygen vacancies [17]. In the case of, the blue shift observed for La doped NiO NPs than the NiO NPs, this shift may be Lanthanum ion are occupation of the substitutional $La_{Ni}$and interstitial La_I sites. The ionic radius of La^{3+} ions (1.061 Å) is higher than the size of the Ni^{2+} ions (0.73 Å), leads to the microstrain values are increased in NiO NPs at La doping by occupying La_{Ni} sites, this effects reduces the PL emission. From the optoelectronic application generally depends on reduction in defect level, which in mainly influenced by electron phonon coupling interaction. In the present work, the

La doped NiO NPs emission decreased as compared to NiO NPs, this results strong support for the further development of wide-range of optical and electrical device application.

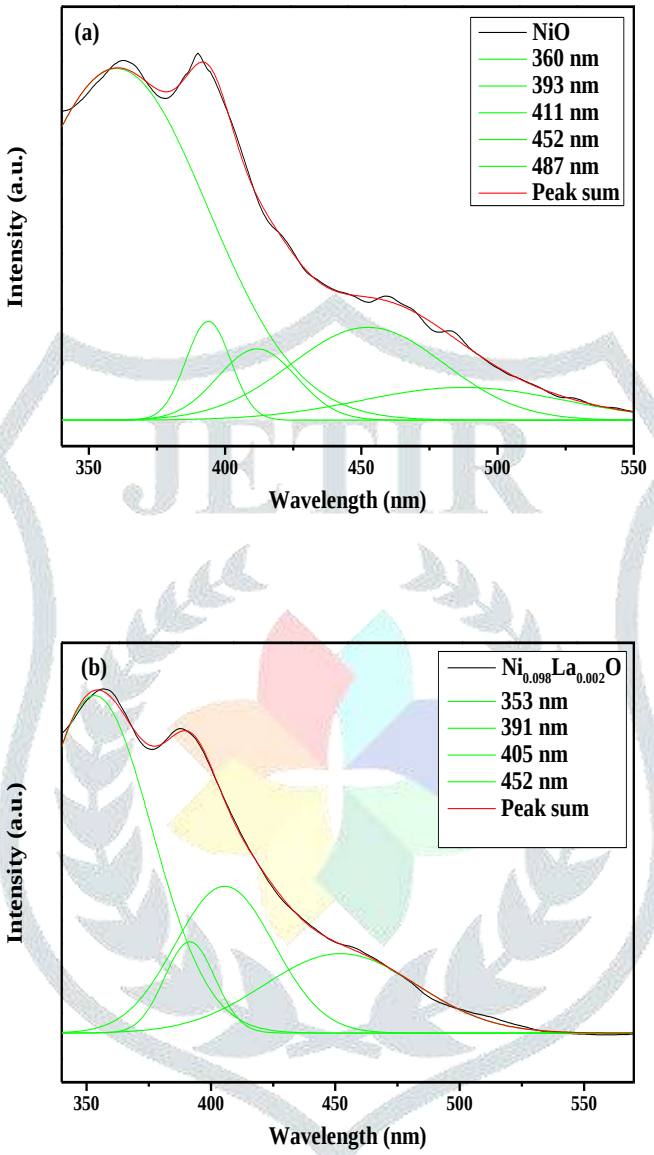

Figure 9 PL spectra of (a) NiO and (b) La doped NiO NPs

IV Conclusions

In the summary, the NiO and Rare earth metal Lanthanum doped NiO NPs were synthesized through green method using *A. indica* leaf phytochemical constituent. The synthesized NiO and La doped NiO NPs average size of particles are estimated at 57.12 nm and 47.72 nm respectively, this result confirmed that enhanced the surface area of La doped NiO NPs than the NiO NPs. The oxidation state of Ni (2p), La (3d)

and O (1s) and composition were identified by XPS spectra. In the FESEM results, the La doped NiO NPs has a more porous present than NiO NPs, more porous formation of La doped NiO NPs surely used in hazardous gas sensing applications. Functional characteristics bands were identified by FTIR measurements. From the PL spectra, the La doped NiO NPs emission values decreased as compared to NiO NPs, these results strongly support for the further development of wide-range of sensor device applications.

References

[1] Singhal G, Bhavesh R, Kasariya K, Sharma AR, Singh RP. 2011. Biosynthesis of silver nanoparticles using Ocimum sanctum (Tulsi) leaf extract and screening its antimicrobial activity. Journal of Nanoparticle Research. 1;13(7):2981-8.

[2] Chen HL, Lu YM, Hwang WS. 2005. Characterization of sputtered NiO thin films. Surface and Coatings Technology. 1;198(1-3):138-42.

[3] Anandan K, Rajendran V. 2011. Morphological and size effects of NiO nanoparticles via solvothermal process and their optical properties. Materials Science in Semiconductor Processing. 1;14(1):43-7.

[4] Zhu G, Xi C, Xu H, Zheng D, Liu Y, Xu X, Shen X. 2012. Hierarchical NiO hollow microspheres assembled from nanosheet-stacked nanoparticles and their application in a gas sensor. RSC Advances. ;2(10):4236-41.

[5] Yayapao O, Thongtem T, Phuruangrat A, Thongtem S. 2013. Sonochemical synthesis of Dy-doped ZnO nanostructures and their photocatalytic properties. Journal of Alloys and Compounds. 5;576:72-9.

[6] Korake PV, Dhabbe RS, Kadam AN, Gaikwad YB, Garadkar KM. 2014. Highly active lanthanum doped ZnO nanorods for photodegradation of metasystox. Journal of Photochemistry and Photobiology B: Biology. 5;130:11-9.

[7] Dash, S. P., Dixit, S., and Sahoo, S., 2017, Phytochemical and Biochemical Characterizations from Leaf Extracts from Azadirachta Indica: An Important Medicinal Plant, Biochem Anal Biochem, 6:2.

[8] Williamson GK, Hall WH. 953, X-ray line broadening from filed aluminium and wolfram. Acta metallurgica. 1;1(1):22-31.

[9] Lin Y, He L, Chen T, Zhou D, Wu L, Hou X, Zheng C. 2018. Cost-effective and environmentally friendly synthesis of 3D Ni 2 P from scrap nickel for highly efficient hydrogen evolution in both acidic and alkaline media. Journal of Materials Chemistry A. 6(9):4088-94.

[10] Kruefu V, Wisitsoraat A, Phokharatkul D, Tuantranont A, Phanichphant S. 2016. Enhancement of p-type gas-sensing performances of NiO nanoparticles prepared by precipitation with RuO2 impregnation. Sensors and Actuators B: Chemical. 29;236:466-73.

[11] M.S. Hamdan, Riyanto, M.R. Othman, 2013. Preparation and Characterization of Nano Size NiOOH, by Direct Electrochemical Oxidation of Nickel Plate, Int. J. Electrochem. Sci., 8,4747 -4760.

[12] Zhang Y, Zhou J, Si J. 2017. Synergistic catalysis of nano-Pd and nano rare-earth oxide/AC: complex nanostructured catalysts fabricated by a photochemical route for selective hydrogenation of phenol. RSC Advances. 7(86):54779-88.

[13] Gawali SR, Patil VL, Deonikar VG, Patil SS, Patil DR, Patil PS, Pant J. 2018. Ce doped NiO nanoparticles as selective NO_2 gas sensor. Journal of Physics and Chemistry of Solids. 114:28-35.

[14] Kundu M, Karunakaran G, Kuznetsov D. 2017. Green synthesis of NiO nanostructured materials using Hydrangea paniculata flower extracts and their efficient application as supercapacitor electrodes. Powder Technology. 15;311:132-6.

[15] Karthikeyan B, Pandiyarajan T, Hariharan S, Ollakkan MS. 2016. Wet chemical synthesis of diameter tuned NiO microrods: microstructural, optical and optical power limiting applications. CrystEngComm. 18(4):601-7.

[16] Agrawal S, Parveen A, Azam A. 2017. Microwave assisted synthesis of Co doped NiO nanoparticles and its fluorescence properties. Journal of Luminescence. 184:250-5.

[17] Umaralikhan L, Jaffar MJ. (2018) X-ray Broadening and Optical Properties of NiO Nanoparticles Prepared via Co-precipitation Method by Varying Temperature. Iranian Journal of Science and Technology, Transactions A: Science.1-4.

[18] Umaralikhan L, Jaffar MJ. 2016. Antibacterial and anticancer properties of NiO nanoparticles by co-precipitation method. Journal of Advanced Applied Scientific Research. Sep 5;1(4):24-35.